

Jasmine Rüegg, Ralf Schumacher, Franz E Weber and Michael de Wild*

Mechanical anisotropy of titanium scaffolds

Numerical simulation and biomechanical verification of anisotropic titanium scaffolds

Abstract: The clinical performance of an implant, e.g. for the treatment of large bone defects, depends on the implant material, anchorage, surface topography and chemistry, but also on the mechanical properties, like the stiffness. The latter can be adapted by the porosity. Whereas foams show isotropic mechanical properties, digitally modelled scaffolds can be designed with anisotropic behaviour. In this study, we designed and produced 3D scaffolds based on an orthogonal architecture and studied its angle-dependent stiffness. The aim was to produce scaffolds with different orientations of the microarchitecture by selective laser melting and compare the angle-specific mechanical behaviour with an in-silico simulation. The anisotropic characteristics of open-porous implants and technical limitations of the production process were studied.

Keywords: Porous metallic scaffold, anisotropy, structure, biomechanical testing

<https://doi.org/10.1515/cdbme-2017-0127>

1 Introduction

While titanium is an established biomaterial and has been used for the production of implant since decades, the ideal geometry and hence biomechanical behaviour is still under discussion. Effects like stress-shielding [1] are the consequences of a mechanical mismatch between the stiff implant material and the softer surrounding bone tissue with

negative impact on the naturally occurring bone remodelling yielding in a further weakening of the bone. In many spinal and cranio-maxillofacial applications, the mechanical stresses are essentially directed along a specific axis and an anisotropic response from the implant or scaffold would be advantageous. The stiffness of implants can be reduced by applying open-porous materials [2] mechanically matching the stiffness of cancellous bone. Porous metallic foams can be tailored by adapting the porosity, however they exhibit isotropic mechanical properties [3]. The improvement of additive manufacturing methods allow the realisation of digitally modelled scaffolds that are designed for anisotropic behaviour. The exact architecture of the porous lattice structures lead to design-specific stiffness and osteoconduction [4,5] and theoretically also to an angle-dependent stiffness [6,7]. In this study, open-porous titanium scaffold of orthogonal microarchitecture with four different spatial orientations were produced by selective laser melting. The angle-dependent mechanical properties were then compared with numerical FE-simulation. The scaffolds were produced in two different scales in order to study the anisotropic characteristics and technical limitations of the production process.

2 Material and methods


2.1 Sample design

Cubic porous sample of two different sizes termed *small* and, scaled by a factor of three, *large* were designed. The structures consist of a porous lattice based on orthogonal struts that fills out the entire cube, see Figure 2a. The unit cells of the scaffolds were modelled with the computer aided design tool (Solidworks 2013). The architecture consists of orthogonal struts of $s = 0.2$ mm (*small*), resp. 0.7 mm (*large*) thickness that are separated by 0.9 mm, resp. 2.7 mm leading to interconnected channels of diameter $c = 0.7$ mm, resp. 2.1 mm (see Table 1 and Figure 2a). Before the subsequent production of the entire scaffolds by selective laser melting (see Figure 2b), the unit cell design were imported in a data preparation and STL editor software for Additive

*Corresponding author: **Michael de Wild:** University of Applied Sciences Northwestern Switzerland, FHNW, School of Life Sciences, Institute for Medical and Analytical Technologies, Gründenstrasse 40, CH-4132 Muttenz, Switzerland, e-mail: michael.dewild@fhnw.ch

Jasmine Rüegg, Ralf Schumacher: University of Applied Sciences Northwestern Switzerland, FHNW, School of Life Sciences, Institute for Medical and Analytical Technologies, Gründenstrasse 40, CH-4132 Muttenz, Switzerland

Franz E Weber: Universität Zürich, Zentrum für Zahnmedizin/MKG, Oral Biotechnology & Bioengineering, Plattenstrasse 11, 8032 Zürich, Switzerland

Open Access. © 2017 Jasmine Rüegg et al., published by De Gruyter.  This work is licensed under the Creative Commons Attribution-NonCommercial-NoDerivatives 4.0 License.

Manufacturing (Magics V.19.02). The above designed unit cells were expanded to 6^3 arrays (in all three room-directions) and then rotated around the main axis by 0° , 15° , 30° or 45° . Finally, all designs with different inclination angles θ were provided with solid endplates on top and on bottom for a defined load application during mechanical testing, see Figure 2c.

Table 1: Structural scaffold parameters

	<i>Small scaffolds</i>	<i>Large scaffolds</i>
Architecture	Orthogonal struts	Orthogonal struts
Length of unit cell	0.9 mm	2.7 mm
Strut thickness s	0.2 mm	0.6 mm
Channel width c	0.7 mm	2.1 mm
Orientation θ	0° , 15° , 30° , 45°	0° , 15° , 30° , 45°
Sample size	6 x 6 x 6 unit cells	6 x 6 x 6 unit cells
Dimensions	5.4x5.4x5.4 mm ³	16.2x16.2x16.2 mm ³
Volume	157 mm ³	4252 mm ³

2.2 Sample production

The scaffolds were produced by additive manufacturing (SLM Solutions 250^{HL}) out of titanium grade II powder with a d_{50} -value of 60 μm . The SLM used a continuous wave 200 W Ytterbium fiber laser with a wavelength between 1068 and 1095 nm that scans the powder bed and solidifies the radiated titanium particles. The layer thickness for both scaffold types was 30 μm .

2.3 Sample preparation

After the SLM production, the scaffolds were cut off the building platform. The base plate of the scaffolds were cleaned from attached support and were treated with sand paper to obtain flat and parallel endplates. The scaffolds were blown out with pressured air and treated by ultrasound to remove remaining powder. The samples for SEM analysis were embedded in a cold polymerizing polymer (Technovit 4071, Kulzer Heraeus), and ground with a series of sandpaper (Struers Silicon carbide grinding paper grit 120, 360 and 580) to obtain a microsection through the sample.

2.4 Structure-mechanical simulation

The linear elastic behaviour of the scaffolds with different orientations of the orthogonal lattice (0° , 15° , 30° and 45°) under uniaxial compression between the two endplates was numerical simulated by COMSOL Multiphysics (Stockholm Sweden, version 5.0). Details can be found in (Zimmermann 2015).

2.5 Mechanical testing

The mechanical stiffness of the scaffolds was determined under compressive loading conditions. With the help of a uniaxial compressive testing machine (Z100 Zwick GmbH & Co) equipped with a laser extensometer for optical strain measurement the Young's Modulus of the scaffolds were determined. The tests were performed strain-controlled with a test speed of 0.005 s^{-1} . The scaffolds were placed between two hard metal plates of a guided pressure unit in order to avoid shear forces. For every sample, a stress strain diagram was obtained and the Young's modulus was determined as the regression line in the linear elastic range between 14 N and 262 N for *small* scaffolds, resp. between 0.26 kN and 5.5 kN for *large* scaffolds.

2.6 SEM analysis

The Scanning Electron Microscope (SEM) TM3030 Plus (Acceleration voltage $U_0 = 15 \text{ kV}$, backscattered electron and secondary electron detectors, Hitachi, Japan) enables the analysis of the scaffolds geometry in the micrometre range.

3 Results

3.1 Sample production

The *small* scaffolds were produced layer-by-layer in an upright position on fine support structures connected to the building platform. As the loose, unmolten titanium powder around the components has a lower thermal heat conductivity than fused solid parts, the positioning of the structure on the building platform is essential. Therefore, the *large* scaffolds were produced in an orientation tilted 20° around the x- and y-axis (see Figure 1). This positioning on the scaffolds corner assures an optimized heat dissipation of the laser-induced energy during the SLM production process. This is important in particular during the fabrication of constructional

transitions e.g. when the active building layers change from the porous support structures to the solid endplates (Figure 1). In this 20°-angled orientation, the massive square element is not generated directly as a singular quadratic area but is gradually growing with each additional layer. Therefore, the introduced thermal energy is continuously dissipated along the underlying solid structures to the building platform. The designed and produced *small* and *large* samples are shown in Figure 2.

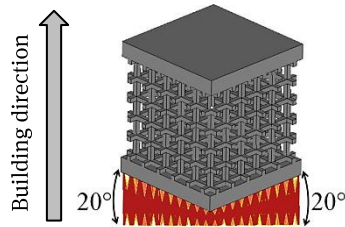


Figure 1: Orientation of the *large* scaffolds on the building platform during SLM-production.

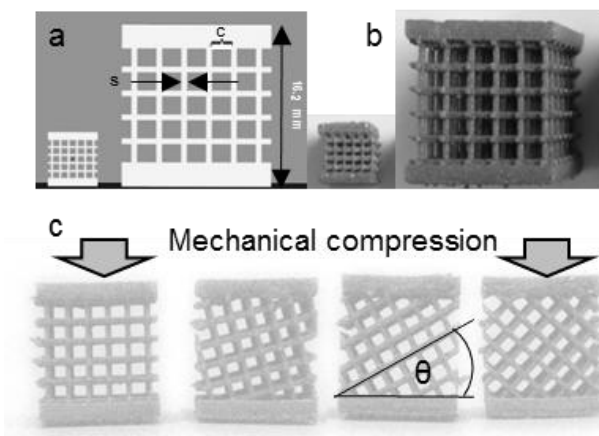


Figure 2: a) Designed and b) produced *small* and *large* scaffolds with $\theta = 0^\circ$. c) Design of samples with inclinations $\theta = 0^\circ, 15^\circ, 30^\circ$ and 45° .

3.2 SEM analysis

The thickness of the struts and the diameter of the channels were determined in SEM images of cross section of embedded samples, see Figure 3 for the *small* scaffolds and Figure 4 for the *large* scaffolds. Vertical and horizontal struts were characterized separately see Table 2.

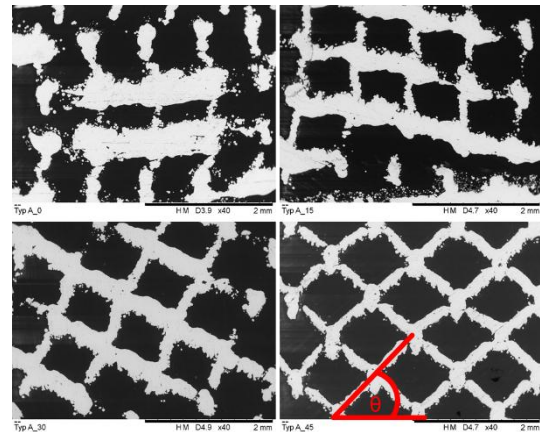


Figure 3: SEM image of the *small* scaffolds (40x magnification) with lattice orientations $\theta = 0^\circ, 15^\circ, 30^\circ$ and 45° .

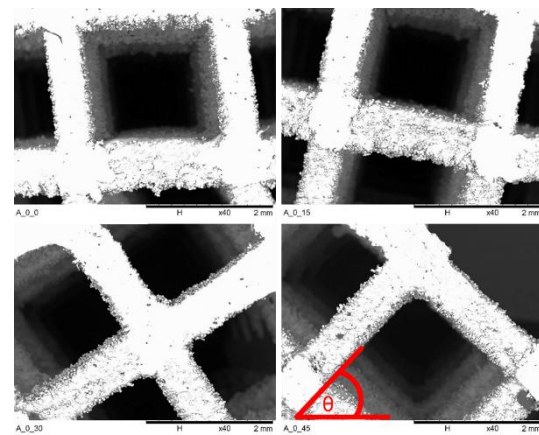


Figure 4: SEM image of the *large* scaffolds (40x magnification) with lattice orientations $\theta = 0^\circ, 15^\circ, 30^\circ$ and 45° .

Whereas the struts of the *large* scaffolds generally are three times thicker than the struts of the *small* scaffolds, we observed significant difference between horizontally and vertically produced struts of the *small* samples, see Table 2. The rod thickness of the *small* scaffolds is at the lower limit of the production specification of the SLM machine, which is reflected in the deviations of the planned strut thickness from the measured strut thickness. In particular, for the angles of $0^\circ, 15^\circ$ and 30° the horizontal struts are considerably larger than designed and result in a reduced vertical/horizontal thickness ratio. The reason for this inhomogeneity lies in the layer-by-layer production process: The vertical struts are created within several layers by reiterated melting steps. As the surrounding powder has a significantly lower thermal conductivity compared to the already fabricated solid struts, the thermal energy of the laser is dissipated to the building platform that acts as a heat sink. On the other hand, the creation of a horizontal strut is completely different from the thermodynamic perspective of the laser process: a laser

trajectory needs to be applied in a new powder layer with no underlying struts. Heat flow is considered to be reduced and higher temperatures are expected around the horizontal strut during laser irradiation. These higher temperatures will cause an expanded melting zone and hence, yield thicker horizontal struts. On the contrary, the 45° oriented struts are again produced under symmetric condition and the vertical/horizontal thickness ratio is closer to unity, see Figure 3 and Table 2.

For the *large* scaffolds the difference between the diameter of the horizontal and vertical struts are less pronounced because the heat-conducting beams are thicker and thus the effects of the heat-affected zone are reduced.

Table 2: Designed and measured strut thicknesses of both scaffold sizes

	Orientation θ [°]	Vertical struts s [μm]		Horizontal struts s [μm]		ratio Vertica l/Horiz ontal
		measured	designed	measured	designed	
Small scaffolds	0	295 ± 23	200	519 ± 119	200	0.57
	15	168 ± 26	200	435 ± 50	200	0.39
	30	245 ± 39	200	388 ± 18	200	0.63
	45	231 ± 34	200	204 ± 21	200	1.14
Large scaffolds	0	542 ± 4	600	720 ± 50	600	0.75
	15	603 ± 20	600	709 ± 20	600	0.85
	30	670 ± 21	600	640 ± 21	600	1.05
	45	642 ± 57	600	701 ± 18	600	0.92

3.3 Comparison between biomechanical and numerical analysis

The calculated Young's modulus, as well as the measured stiffness of the *small* and *large* scaffolds were normalized (to the softest specimen of the series) and are depicted in Figure 5 as a function of the lattice rotation angle. The *large* scaffolds show the expected trend: An increased rotation angle leads to softer structures as expected by the less direct load transfer through the struts, see Figure 5. On the other hand, it is obvious that the *small* scaffolds did not reproduce the numerical stiffness values empirically.

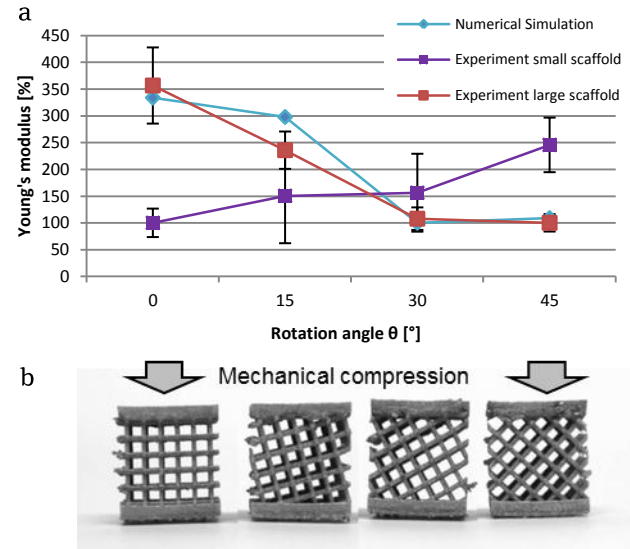


Figure 5: a) Angle-dependent stiffness of *large* (red) and *small* (purple) scaffolds derived by numerical simulation (light blue diamonds) and mechanical testing (squares). b) Photo of *large* scaffolds with lattice orientations $\theta = 0^\circ, 15^\circ, 30^\circ$ and 45° .

4 Conclusion

The accurately produced *large* titanium samples with the defined lattice geometry show the theoretically expected angle-dependence of the lattice structure. It is therefore possible to design open-porous implants with anisotropic mechanical stiffness. This opens new perspectives to create smart implants that react different towards specific directions and tissues: Whereas it is relatively stiff in normal 0° direction, the implant acts rather soft when loaded under 45° and the surrounding tissue is stimulated differently.

The down-scaling of the SLM production process, however, is limited by process factors like the minimal diameter of the powder particles, the focus spot of the laser, the layer thickness and also by geometric factors like thickness and orientation of the structure relative to the powder bed. The fabrication of horizontal structures ($\theta = 0^\circ$ samples) in the powder bed is critical due to heat accumulation. As a result, irregular rod thickness and unexpected mechanical behaviour were observed. Note that this is the reason why the samples were produced in a 20° tilted orientation, see Figure 1.

Author's Statement

Research funding: This study was kindly supported by Swiss National Science Foundation (31003A_140868). **Conflict of interest:** Authors state no conflict of interest. **Material and Methods:** Informed consent: Informed consent is not

applicable. Ethical approval: The conducted research is not related to either human or animals use.

References

- [1] Srinivasan P et al. Strain shielding in trabecular bone at the tibial cement-bone interface. *J Mech Behav Biomed Mater.* 2017;66:181-186.
- [2] Helsen JA, Breme HJ. *Metals as Biomaterials.* 1998.
- [3] Imwinkelried T. Mechanical properties of open-pore titanium foam. *J Biomed Mater Res A.* 2007;81(4):964-70.
- [4] de Wild M et al. Influence of Microarchitecture on Osteoconduction and Mechanics of Porous Titanium Scaffolds Generated by Selective Laser Melting. *3D Printing and Additive Manufacturing.* 2016;3(3):142-151.
- [5] de Wild M et al. Bone regeneration by the osteoconductivity of porous titanium implants manufactured by selective laser melting: A histological and μ CT study in the rabbit. *Tissue Engineering Part A.* (2013);19(23-24):2645-2654.
- [6] Zimmermann S, de Wild M. Density- and Angle-Dependent Stiffness of Titanium 3D Lattice Structures. *BioNanoMat.* 2014;15(S1):S35.
- [7] Zimmermann S et al. Stiffness-anisotropy of porous implant geometries. *Europ Cells and Mat.* 2015;29(Suppl. 2):22.